

# The efficacy of novel heterocyclic activators against mercuric chloride-induced acute renal failure in rats

Safaa H. Mohamed<sup>1\*</sup> , Dina S. El-Kady<sup>1</sup>, Gamal A. ElMegeed<sup>1</sup>, Mahitab I. El-kassaby<sup>2</sup>, Abdel-Razik H. Farrag<sup>3</sup>, Mervat M. Abdelhalim<sup>1</sup>, Naglaa A. Ali<sup>1</sup>

<sup>1</sup>Hormones Department, Medical Research and Clinical Studies Institute, National Research Centre, Giza, Egypt.

<sup>2</sup>Medical Physiology Department, Medical Research and Clinical Studies Institute, National Research Centre, Giza, Egypt.

<sup>3</sup>Departments of Pathology, Medical Research and Clinical Studies Institute, Giza, Egypt.

## ARTICLE INFO

Received on: 26/09/2022  
Accepted on: 07/01/2023  
Available Online: 28/03/2023

### Key words:

Heterocyclic, steroids,  
mercuric chloride, kidney  
injury, inflammation.

## ABSTRACT

Mercury chloride (HgCl<sub>2</sub>) has a potent nephrotoxic effect. Synthesizing new heterocyclic steroids using some chemical strategies could be predictable to have promising efficiency against mercuric chloride-induced acute renal failure. Analytical and spectral data affirmed the structure of the unprecedented heterocyclic steroids. To assess their biological activities, rats were treated with tested compounds after HgCl<sub>2</sub> was intraperitoneally injected, a daily treatment for another 1 month. In comparison to the HgCl<sub>2</sub> group, synthesized compounds significantly prevented increased serum levels of creatinine, urea, renal lipid peroxidation, and nitric oxide levels, decreasing serum glutamic oxaloacetic transaminase, glutamic pyruvic transaminase, alkaline phosphatase, tumor necrosis factor- $\alpha$ , and interleukin-1  $\beta$  levels and lipid profile concentration, and showed a significant increase in high-density lipoprotein and catalase levels. They, moreover, upregulated levels of Nephren-2 and KIM-1 genes' expression. Histopathological results supported our biochemical findings. Noteworthy, compounds 6 and 9 in particular have more antioxidant and anti-inflammatory activities than compounds 4 and 5 and play a salutary role against HgCl<sub>2</sub> toxicity. The biological characteristics of these new generations of heterocyclic steroid derivatives, which are demonstrated by their anti-inflammatory and antioxidant properties, could serve as a useful framework for the continued development of potent therapeutics.

## INTRODUCTION

Mercury (Hg) is a toxic element present in the earth's crust and assorted among the most serious environmental hazards. Humans are at risk of Hg in air, water, and polluted food (Balali-Mood *et al.*, 2021) and inorganic and organic forms for natural or human bounces, cultivation, exaggeration of cosmetic or therapeutic agents, and remnant fuel releases (Pollard *et al.*, 2019). Exposure to Hg produces detrimental effects, like nephrotoxicity, pulmonary diseases, vomiting, hypertension, nausea, reproductive dysfunctions, and neurotoxicity (Balali-Mood *et al.*, 2021). Kidneys are the organs most affected by mercury, developing

renal damage where the cellular antioxidant system is disturbed and the elaboration of oxidative stress, such as superoxide hydrogen peroxide, anion radicals, and hydroxyl radicals, which subsequently improved levels of reactive oxygen species (ROS) lipid, protein, and DNA oxidation has occurred by a forces affinity of Hg to molecules in sulfhydryl group as glutathione (Hosseini *et al.*, 2018). Moreover, mercuric chloride (HgCl<sub>2</sub>) with protein forms organomercury complexes mainly on getting methylated to methyl mercury compounds which have the ability to accumulate in target organs principally kidneys and brain (Joshi *et al.*, 2017).

Steroid drugs are an important therapeutic target for the treatment of diseases such as hypogonadism, senile osteoporosis, some types of anemia, liver dysfunction, kidney disease, and psychiatric and behavioral disorders in both sexes as well as other problems with the human body (Dashbaldan *et al.*, 2021). A lot of attention in drug therapies has been given to steroid compounds structural modification by incorporation of hetero

### \*Corresponding Author

Safaa H. Mohamed, Hormones Department, Medical Research and Clinical Studies Institute, National Research Centre, Giza, Egypt.  
E-mail: [rise\\_sun\\_1982@hotmail.com](mailto:rise_sun_1982@hotmail.com)

atoms likely to elucidate the progression of solubility and facilitate salt formation properties, which are major for oral absorption (Yahya *et al.*, 2017).

González *et al.* (2008) showed numerous methods in which steroids are effective in treating chronic renal disorders. Moreover, steroid-treated patients had considerably lower serum creatinine concentrations than untreated individuals. In addition, early steroid therapy and less extensive interstitial fibrosis on biopsy were prognostic of renal recovery.

The goal of this research is to eradicate renal failure by targeting nephrotoxicity using new steroidal heterocyclic derivatives. Through a combination of synthetic and computational studies, the design and synthesis of novel heterocyclic steroids were performed. The antioxidant and anti-inflammatory effects of the new synthesized agents in animal models of renal failure were investigated using biochemical and histopathological as well as molecular analysis system studies.

## MATERIAL AND METHODS

### Chemistry

Onset steroids were purchased from Sigma Company, USA. All solvents were hydrated by distillation before use. All melting points were gauged by an electrothermal apparatus and were uncorrected. The IR spectra were documented in KBr discs on a Shimadzu FT-IR 8,201 PC spectrometer and expressed in  $\text{cm}^{-1}$ . Fourier-transform infrared (FTIR) spectrum is recorded between 4,000 and 400  $\text{cm}^{-1}$ . The  $^1\text{H}$  NMR and  $^{13}\text{C}$  NMR spectra were reported by Joel Instruments (Japan), at 270 and 125 MHz, respectively, in DMSO- $d_6$  as solvent and chemical shifts were notation in ppm relative to TMS. The spin multiplicities were abbreviated by the following letters: *s*-singlet, *d*-doublet, *t*-triplet, quartet and *m* (multiple, more than quartet). Mass spectra were recorded on a GCMS-QP 1,000 EX spectra, mass spectrometer operating at 70 eV. Elemental analyses were held by the Microanalytical Data Unit at the National Research Centre, Giza, Egypt and the Microanalytical Data Unit at Cairo University, Giza, Egypt. The reactions were monitored by thin layer chromatography (TLC) which was carried out using Merck 60 F254 aluminum sheets and visualized by UV light (254 nm). The mixtures were separated by preparative TLC and gravity chromatography. All steroid derivatives showed that the characteristic spectral data of cyclopentanoperhydrophenanthrene nuclei of the androstane series were similar to those reported in the literature (Fuente *et al.*, 2005).

### Synthetic methods and analytical and spectral data *Synthesis of 17-azido-16-formyl-10,13-dimethyl-2,3,4,5,6,7,8,9,10,11,12,13,14,15-tetradecahydro-1H-cyclopenta[a]phenanthren-3-ylacetate (2)*

A mixture of compound **1** (Brief preparation: reaction of 3 $\beta$ -acetoxyandrostane-17-one with phosphorus oxychloride and dimethylformamide gave 3 $\beta$ -acetoxy-17-chloro-16-formyl-5 $\alpha$ -androst-16-ene **1**) (0.05 mmol) and sodium azide (0.06 mmol) in DMSO (15 ml) was stirred at the 110°C for 6 hours. Then, the mixture was poured into water (50 ml); the separated precipitate was combined by filtration and recrystallized from benzene to give

**2**. When the procedure was done at 40°C, 1.3 g of compound **2** as the sole product was produced.

Brown powder from absolute ethanol, Yield = 70%, MP 113°C–115°C. IR (kBr,  $\text{cm}^{-1}$ ):  $\nu$  1,732, 1,646 (C=O) 2,936, 2,858 ( $\text{CH}_2$ ,  $\text{CH}_3$ -aliphatic).  $^1\text{H}$  NMR (DMSO- $d_6$ , ppm):  $\delta$  = 0.81 (*s*, 3H,  $\text{CH}_3$ -18), 1.00–2.12 (*m*, steroid moiety), 1.24 (*s*, 3H,  $\text{CH}_3$ -19), 2.01 (*s*, 3H,  $\text{CH}_3$ -acetate), 4.60 (*q*, 1H,  $\text{C}_3$ -H), 10.18 (*d*, 1H, aldehyde group).  $^{13}\text{C}$  NMR (DMSO- $d_6$ , ppm):  $\delta$  = 36.33 (C-1), 28.37 (C-2), 73.27 (C-3), 34.35 (C-4), 44.46 (C-5), 27.57 (C-6), 31.13 (C-7), 33.75 (C-8), 53.89 (C-9), 36.33 (C-10), 21.00 (C-11), 35.73 (C-12), 43.87 (C-13), 47.67 (C-14), 33.48 (C-15), 150.60 (C-16), 165.00 (C-17), 20.82 (C-18), 17.01 (C-19), 170.20, 186.20 (C=O), 20.64 (C methyl). MS (EI)  $m/z$  = 385 [ $\text{M}^+$ , 5%], 375 (63), 360 (100), 232 (55), 315 (14), 282 (20), 275 (15). Call for  $\text{C}_{22}\text{H}_{31}\text{N}_3\text{O}_3$  (385.23).

### *Synthesis of 10-amino-6a, 8a-dimethyl-1,2,2a, 3,4,5,6,6a, 6b,7,8,8a, 10,12,12a, 12 b-hexadecahydronaphtho[2', 1': 4,5]indeno[1,2-c] pyrazol-4-ylacetate (3)*

Under reflux in ethanol (125 ml), a mixture of compound **2** (0.03 mmol), hydrazine hydrate (25 ml), and acetic acid (2 ml) was heated for 18 hours. The cold mixture gave output pyrazole derivative **3** after being poured into water.

Gray powder from absolute ethanol, Yield = 25%, MP 160°C. IR (kBr,  $\text{cm}^{-1}$ ):  $\nu$  3,423 ( $\text{NH}_2$ ) 2,937, 2,859 ( $\text{CH}_2$ ,  $\text{CH}_3$ -aliphatic).  $^1\text{H}$  NMR (DMSO- $d_6$ , ppm):  $\delta$  = 0.89 (*s*, 3H,  $\text{CH}_3$ -18), 1.00–2.30 (*m*, steroid moiety), 1.27 (*s*, 3H,  $\text{CH}_3$ -19), 2.01 (*s*, 3H,  $\text{CH}_3$ -acetate), 4.60 (*q*, 1H,  $\text{C}_3$ -H), 7.10 (*s*, 1H,  $\text{NH}$ ,  $\text{D}_2\text{O}$  exchangeable), 8.40 (*s*, 1H, CH-pyrazole ring). MS (EI)  $m/z$  = 372 [ $\text{M}^+$ , 55%], 356 (17), 318 (39), 281 (40). Call for  $\text{C}_{22}\text{H}_{33}\text{N}_3\text{O}_2$  (371.52).

### *Synthesis of 6a, 8a-dimethyl-1,2,2a, 3,4,5,6,6a, 6b,7,8,8a,9, 12,12a, 12 b-hexadecahydronaphtho[2', 1': 4,5]indeno[1,2-c] pyrazol-4-yl acetate (4)*

A mixture of compound **2** (0.02 mmol) and hydrazine hydrate (2.8 g) in ethanol (50 ml) with a crystal of iodine was set aside at room temperature for 2 hours. A yellow precipitate yield when the mixture was poured into water (200 ml) was obtained by filtration.

White powder from absolute ethanol, Yield = 45%, MP 160°C–162°C. IR (kBr,  $\text{cm}^{-1}$ ):  $\nu$  3,426 ( $\text{NH}$ ) 2,937, 2,858 ( $\text{CH}_2$ ,  $\text{CH}_3$ -aliphatic), 1,732 (C=O).  $^1\text{H}$  NMR (DMSO- $d_6$ , ppm):  $\delta$  = 0.84 (*s*, 3H,  $\text{CH}_3$ -18), 1.06–2.37 (*m*, steroid moiety), 1.36 (*s*, 3H,  $\text{CH}_3$ -19), 2.40 (*s*, 3H,  $\text{CH}_3$ -acetate), 4.57 (*q*, 1H,  $\text{C}_3$ -H), 8.30 (*s*, 2H,  $\text{NH}_2$ ,  $\text{D}_2\text{O}$  exchangeable). MS (EI)  $m/z$  = 357 [ $\text{M}^+$ , 42%], 344 (15), 332 (16), 297 (5), 296 (42). Call for  $\text{C}_{23}\text{H}_{32}\text{N}_2\text{O}_2$  (356.51).

### *Synthesis of 9-carbamothioyl-6a, 8a-dimethyl-1,2,2a, 3,4,5,6,6a, 6b,7,8,8a, 9,12,12a, 12 b-hexadecahydronaphtho[2', 1': 4,5]indeno[1,2-c] pyrazol-4-ylacetate (5)*

An equimolar mixture of 17-chloro-16-formyl-androstane ester (**1**) (0.143 mmol) and thiosemicarbazide (0.143 mmol) in ethanol (25 ml) and sodium acetate (0.07 mmol) was refluxed for 8 hours. The solid separated was filtered, dried, and crystallized using ethanol Dimethylformamide (DMF) mixtures to give compound **5**.

White powder from ethanol DMF mixture, Yield = 78%, MP 284°C–286°C. IR (kBr,  $\text{cm}^{-1}$ ):  $\nu$  2,389 ( $\text{NH}_2$ ), 1,734 (C=O) 2,930, 2,853 ( $\text{CH}_2$ -aliphatic), 1,244–1,002 (C=S).  $^1\text{H}$  NMR

(DMSO- $d_6$ , ppm):  $\delta$  = 0.81 (*s*, 3H, CH<sub>3</sub>-18), 1.96–2.51 (*m*, steroid moiety), 1.35 (*s*, 3H, CH<sub>3</sub>-19), 3.30 (*s*, 3H, CH<sub>3</sub>-acetate), 4.61 (*q*, 1H, C<sub>3</sub>-H), 6.60 (*s*, 1H, CH-pyrazole ring), 11.36 (*s*, 2H, NH<sub>2</sub>, D<sub>2</sub>O exchangeable). MS (EI)  $m/z$  = 416 [ $M^+$ , 59%], 300 (54), 313 (36), 280 (100). Call for C<sub>31</sub>H<sub>37</sub>N<sub>3</sub>O<sub>2</sub>S (415.59).

**Synthesis of 6a, 8a-dimethyl-9-(4-phenylthiazol-2-yl)-1,2,2a,3,4,5,6,6a, 6b,7,8,8a, 9,12,12a, 12 b-hexadecahydronaphtho[2', 1': 4,5]indeno[1,2-c] pyrazol-4-ylacetate (6)**

An equimolar mixture of **5** (0.01 mmol) and substituted phenacyl bromide (0.01 mmol) in ethanol was refluxed for 4 hours. After completion of the reaction, the reaction mixture was left to cool. Thus, the solid was separated by filtration and crystallized using ethanol DMF mixtures.

Pale green powder from ethanol/DMF mixture, Yield = 62%, MP 131°C–133°C. IR (kBr, cm<sup>-1</sup>):  $\nu$  1,726 (C=O) 2,930, 2,853 (CH<sub>2</sub>-aliphatic). <sup>1</sup>H NMR (DMSO- $d_6$ , ppm):  $\delta$  = 0.85 (*s*, 3H, CH<sub>3</sub>-18), 1.21–2.27 (*m*, steroid moiety), 1.31 (*s*, 3H, CH<sub>3</sub>-19), 2.40 (*s*, 3H, CH<sub>3</sub>-acetate), 4.60 (*q*, 1H, C<sub>3</sub>-H), 7.36 (*s*, 1H, CH-pyrazole ring), 7.96 (*s*, 1H, CH-thiazole ring), 7.92 (*m*, aromatic hydrogen). <sup>13</sup>C NMR (DMSO- $d_6$ , ppm):  $\delta$  = 36.66 (C-1), 30.70 (C-2), 82.29(C-3), 34.38 (C-4), 47.73 (C-5), 27.59 (C-6), 31.19 (C-7), 34.68 (C-8), 53.70 (C-9), 36.66 (C-10), 20.65 (C-11), 33.50 (C-12), 42.54 (C-13), 53.50 (C-14), 23.46 (C-15), 124.00 (C-16), 140.45 (C-17), 19.08 (C-18), 12.35 (C-19), 128.70, 129.10, 129.30, 129.90 (C aromatic), 170.77, 171.20 (2C=O), 130.17 (C-diazole), 113.20, 146.00, 152.10 (3C-thiazole), 21.32 (C methyl). MS (EI)  $m/z$  = 515 [ $M^+$ , 32%], 438 (3), 335 (11), 314 (9), 201 (8), 160 (2). Call for C<sub>31</sub>H<sub>37</sub>N<sub>3</sub>O<sub>2</sub>S (515.71).

**Synthesis of 8R,9S, 10R,13S, 14S, 17S, E)-10,13-dimethyl-3-(phenylimino)-2,3,6,7,8,9,10,11,12,13,14,15,16, 17-tetradecahydro-1H-cyclopenta[a] phenanthren-17-yl acetate (8)**

Acetylated testosterone **7** (0.01 mmol) was fused with aniline (0.01 mmol) for 30 minutes and then 25 ml of absolute ethanol was added to the reaction mixture. The reaction mixture was refluxed for 6–8 hours and then cooled to room temperature. The separated solid was filtered, washed with water, and recrystallized from benzene to give a steroidal amino derivative **8**.

Dark brown powder from benzene, Yield = 71%, MP 72°C–74°C. IR (kBr, cm<sup>-1</sup>):  $\nu$  2,942, 2,836 (CH<sub>2</sub>, CH<sub>3</sub>-aliphatic), 1,730 (C=O). <sup>1</sup>H NMR (DMSO- $d_6$ , ppm):  $\delta$  = 0.90 (*s*, 3H, CH<sub>3</sub>-18), 1.30–2.35 (*m*, steroid moiety), 1.05 (*s*, 3H, CH<sub>3</sub>-19), 2.49 (*s*, 3H, CH<sub>3</sub>-acetate), 4.60 (*q*, 1H, C<sub>17</sub>-H), 5.60 (*s*, 1H, C<sub>4</sub>-H), 6.90–7.40(*m*, aromatic-H). MS (EI)  $m/z$  = 405 [ $M^+$ , 3%], 329 (14), 305 (69), 348 (5), 313 (1), 253 (34), 146 (47). Call for C<sub>27</sub>H<sub>35</sub>N<sub>2</sub>O<sub>2</sub> (405.26).

**Synthesis of (8'R,9'S,10'R,13'S,14'S,17'S)-3-chloro-10',13'-dimethyl-4-oxo-1-phenyl-1',2',6',7',8',9',10',11',12',13',14', 15',16',17'-tetradecahydrospiro[azetidine-2,3'-cyclopenta[a] phenanthren]-17'-ylacetate (9)**

Steroidal amino derivative **8** was dissolved in 30 ml of dichloromethane and added to this solution; chloroacetyl chloride and a few drops of triethylamine were added. Then the reaction mixture was refluxed for 3–3.5 hours. The progress as well as completion of the reaction was monitored by TLC. After completion of the reaction, the solvent was put under reduced pressure to give azetidine derivative **9**.

Black powder from absolute ethanol, Yield = 82%, mp125°C. IR (kBr, cm<sup>-1</sup>):  $\nu$  2,943, 2,748 (CH-aliphatic), 1,685,

1,728 (2 C=O). <sup>1</sup>H NMR (DMSO- $d_6$ , ppm):  $\delta$  = 0.90 (*s*, 3H, CH<sub>3</sub>-18), 1.02–2.17 (*m*, steroid moiety), 1.17 (*s*, 3H, CH<sub>3</sub>-19), 2.49 (*s*, 3H, CH<sub>3</sub>-acetate), 4.26 (*t*, 1H, C<sub>17</sub>-H), 5.50 (*s*, 1H, C<sub>4</sub>-H), 7.20–7.60 (*m*, aromatic-H), 5.20 (*s*, 1H, CH-Cl). <sup>13</sup>C NMR (DMSO- $d_6$ , ppm):  $\delta$  = 27.59 (C-1), 31.44 (C-2), 72.00 (C-3), 66.20 (C-4), 140.45 (C-5), 34.37 (C-6), 31.18 (C-7), 34.67 (C-8), 53.90 (C-9), 36.65 (C-10), 20.64 (C-11), 36.90 (C-12), 42.53 (C-13), 50.78 (C-14), 23.45 (C-15), 27.59 (C-16), 82.29 (C-17), 12.36 (C-18), 19.08 (C-19), 127.28, 129.28, 129.40, 130.16, 139.10 (C aromatic), 161.20, 170.79 (2C=O), 126.50 (C-Cl), 21.33 (C methyl). MS (EI)  $m/z$  = 481 [ $M^+$ , 21%], 404 (5), 467 (22), 101 (23). Call for C<sub>29</sub>H<sub>36</sub>Cl<sub>3</sub>N<sub>3</sub>O<sub>3</sub> (482.06).

## Biological application

### Chemicals

HgCl<sub>2</sub> was purchased from Sigma Chemical COM. It was dissolved in distilled water and intraperitoneally injected (i.p) at a dose of (5 mg/kg) once daily for 30 days. Thiobarbituric was obtained from Fluka (Berlin, Germany). All the other chemicals were of the highest analytical grades, which were commercially available.

### Animals and test conditions

Albino female rats (150 rats), weighing 180–200 g, aged 13–15 weeks, were provided by the Animal House Colony of the National Research Centre, Cairo, Egypt and acclimated for one week in a defined pathogen-free barrier area where the temperature was 25°C ± 1°C and humidity was 55%. Rats were continuously controlled with a 12 hours light/dark cycle in the National Research Centre animal husbandry colony. Rats were housed individually with ad libitum access to a standard laboratory diet and tap water. All animal procedures were performed after approval by the Ethics Committee of the National Research Centre and in accordance with the recommendations for the appropriate care and use of laboratory animals (NIH publication No. 85–23, revised 1985).

### Experimental planning

130 Albino rats were classified into five main groups (10 rats/group). **Group 1:** Normal, healthy animals (10 rats) were considered as negative control. **Group 2:** Acute kidney injury (AKI group) was intraperitoneally injected with HgCl<sub>2</sub> at a dose level of 5 mg/kg b.wt for 1 month (Salman *et al.*, 2016). **Group 3:** It contains healthy animals and is divided into five subgroups in accordance with the tested compounds. Each subgroup daily was given 50 mg/kg b. wt one of the tested compounds (**5, 6, 9, and 4, respectively**) dissolved in DMSO for 1 month (Abeed *et al.*, 2017), so as to confirm the safety of these compounds, serving as positive control groups. **Group 4:** This group was induced AKI and divided also into five subgroups. Each subgroup daily was given 50 mg/kg b. wt one of the tested compounds (**5, 6, 9, and 4, respectively**) dissolved in DMSO for 1 month. **Group 5:** Animals were induced with AKI and treated orally with losartan dissolved in DMSO in a dose of 30 mg/kg daily for another 1 month (Abeed *et al.*, 2017) as a reference drug.

### Sample preparation

24 hours after obtaining HgCl<sub>2</sub>, blood samples were outgoing from rats of all groups via anesthetizing but were euthanized via CO<sub>2</sub> asphyxiation. Serum was used for estimation of serum urea, creatinine, cholesterol, triglyceride, LDL, HDL, GPT,

GOT, ALP, TNF- $\alpha$ , and IL-1  $\beta$  levels, using specific diagnostic kits. Immediately after blood sampling, animals were sacrificed by cervical dislocation under ether anesthesia. The two kidneys from each rat were immediately dissected and rinsed with phosphate-buffered saline (PBS) to remove excess blood. Weighed parts from both kidneys were homogenized (MPW-120 Homogenizer, MED Instruments, Poland) in PBS to obtain 20% homogenate that was stored overnight at  $\leq -20^{\circ}\text{C}$ . After two freeze-thaw cycles were performed to break the cell membranes, the homogenates were centrifuged for 5 minutes at  $5,000 \times g$  using a cooling centrifuge (Sigma and Laborzentrifugen, 2K15, Germany). The supernatant was removed immediately and assayed for CAT, lipid peroxides, measured as MDA, and NO (nitrite and nitrate, stable metabolites of NO) contents using specific commercial reagent kits (Biodiagnostic, Egypt).

## Biochemical assay

### Oxidative stress biomarkers

Renal NO (Catalog No. NO 25 33) level was assayed by the spectrophotometric method according to Berkels *et al.* (2004). LPO products represented by MDA (Catalog No. MD 25 28) were evaluated by the method of Satoh (1978) using the thiobarbituric acid and measuring the reaction product spectrophotometrically (UV-2401PC- SHIMADZU, Japan) at 534 nm. CAT activity in kidney tissue homogenate was determined calorimetrically according to the method of Aebi (1984).

### Lipid profile and liver biomarkers assays

Estimation of serum urea, creatinine, cholesterol, triglyceride, LDL, HDL, GPT, GOT, and ALP levels was determined using Biodiagnostic kits, Dokki, Egypt following the manufacturer's instructions of kits. Serum creatinine (Catalog No. CR12 51) was measured as described by Henry (1974) and urea (Catalog No. 2050) as described by Patton and Crouch (1977). Estimations of GOT (Catalog No. 99 87 20) and GPT (Catalog No. 99 76 10) by the method described by Reitman and Frankel (1957) and ALP (Catalog No. 99 13 20) in serum were carried out by the method of Belfield and Goldberg (1971). Estimation of lipid profile parameters, such as cholesterol (Catalog No. NS 230 001), triglyceride (Catalog No. 2100 CE), LDL (Catalog No. NS 280 001), and HDL (Catalog No. 0599) in serum, was carried out by the method of Fossati and Principe (1982).

### Inflammatory markers

The serum content of TNF- $\alpha$  (Catalog No. ET2010-1) was measured by ELISA (Enzyme-Linked Immunosorbent Assay) (Sorin Biomedica, S.A.S.) kit, according to the manufacturer's instructions of NOVA kit, Beijing, China, for calculating the results. Also, the serum level of i IL-1  $\beta$  was estimated using rat ELISA kits purchased from Elabscience Biotechnology Co., Ltd (P.R.C.), according to the manufacturer's instructions provided with the assay kits.

### Molecular genetics study

#### Molecular analyses for nephrin-2 and KIM-1 genes expression using semi-quantitative real-time PCR

##### Isolation of total RNA

Total RNA was isolated from the brain tissue of female rats by the standard TRIzol<sup>®</sup> reagent extraction method (Invitrogen,

USA). Then, the complete Poly(A) RNA was reversely transcribed into cDNA in a total volume of 20  $\mu\text{l}$  using Revert Aid<sup>™</sup> first strand cDNA synthesis kit (MBI Fermentas, Germany).

##### Semi-quantitative real time-polymerase chain reaction (RT-PCR)

An iQ5-BIO-RAD Cycler (Cepheid, USA) was used to determine the rat cDNA copy number. Polymerase Chain Reaction (PCR) reactions were set up in 25  $\mu\text{l}$  reaction mixtures containing 12.5  $\mu\text{l}$  1  $\times$  SYBR<sup>®</sup> Premix Ex Taq TM (TaKaRa, Biotech. Co. Ltd.), 0.5  $\mu\text{l}$  0.2 M forward primers, 0.5  $\mu\text{l}$  0.2 M reverse primer (Table 1), 6.5  $\mu\text{l}$  distilled water, and 5  $\mu\text{l}$  of cDNA template.

The reaction program: denaturation at  $95.0^{\circ}\text{C}$  for 15 seconds; annealing at  $55.0^{\circ}\text{C}$  for 30 seconds, and extension at  $72.0^{\circ}\text{C}$  for 30 seconds. At the end of each reverse transcriptase PCR (RT-PCR), a melting curve was performed at  $95.0^{\circ}\text{C}$  to check the quality of the used primers. The gene expression was calculated using the formulae of Bio-Rad Laboratories Inc.

##### Histopathological examination

The kidney tissues from all tested groups were fixed in 10% formalin for 1 week, washed in running tap water for 24 hours, and dehydrated in ascending series of ethanol (50%–90%), followed by absolute alcohol. The samples were cleared in xylene and immersed in a mixture of xylene and paraffin at  $60^{\circ}\text{C}$ . The tissue was then transferred to pure paraffin wax of a melting point of  $58^{\circ}\text{C}$  and then mounted in blocks and left at  $4^{\circ}\text{C}$ . The paraffin blocks were sectioned on a microtome at a thickness of 5  $\mu\text{m}$  and mounted on clean glass slides and left in the oven at  $40^{\circ}\text{C}$  to dry. The slides were deparaffinized in xylene and then immersed in descending series of ethanol (90%–50%). The ordinary hematoxylin and eosin (H & E) stain was used to stain the slides (Drury and Wallington, 1980).

### Statistics

In this study, all data were analyzed by one-way analysis of variance using the Statistical Package for the Social Sciences program, version 21, followed by least significant difference to compare the significance between groups (Armitage and Berry, 1987). The difference was considered significant when the  $p$ -value was  $< 0.05$ .

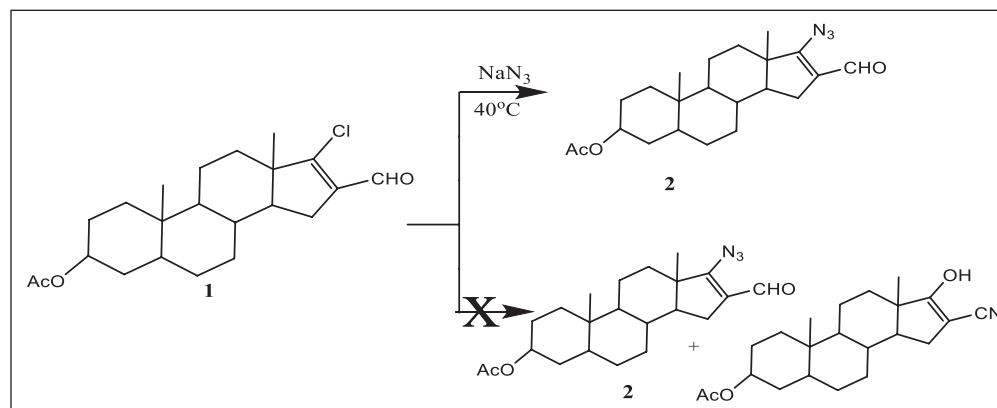
## RESULTS AND DISCUSSION

### Chemistry

Compound **1** was synthesized starting with epiandrosterone as reported in the literature of the previous work of Elmegeed (2004). Treatment of compound **1** with sodium azide at  $40^{\circ}\text{C}$  gave compound **2** as a sole product. Mass Spectra, IR, and  $^1\text{H}$  NMR data confirmed the structure of compound **2** (Scheme 1) (*c.f.* Materials and Methods).

Treated compound **2** accompanied by hydrazine hydrate in the existence of acetic acid in refluxed ethanolic solution yielded the pyrazoloandrostane derivative **3**. However, treatment of compound **2** with hydrazine hydrate at room temperature in the presence of iodine afforded the pyrazoloandrostane derivative **4**.  $^1\text{H}$ NMR spectra show up the subsistence of an NH signal at 7.10 ppm of compound **4** and  $\text{NH}_2$  signal at 8.30 ppm of compound **3** which vanished by deuteration (Scheme 2) (*c.f.* Materials and Methods).

Furthermore, when compound **1** reacted with thiosemi-carbazide it gave pyrazoloandrostane derivative **5**. On the other



**Scheme 1.** Treatment of compound 1 with sodium azide at the 40°C gave compound 2.

hand, the thiazolyl pyrazoloandrostane derivative **6** was obtained in good yield by refluxing compound **5** with phenacyl bromide in ethanol for 8 hours (Scheme 3).

Steroidal imine derivative **8** was prepared by condensing steroidal unsaturated ketone **7** with aniline. Compound **8** was used as the starting material to synthesize the steroid spiroazitidinone **9**. In this work, we examined the synthesis of the steroid spiroazitidinone **9** via a Studdinger chitin-imine [2 + 2] cycloaddition reaction using the androstandroin 4-ene exocyclic variant imines (Scheme 4). The  $^{13}\text{C}$  NMR,  $^1\text{H}$  NMR, IR, and EIMS data for all new compounds are appropriate with the proposition structures (see Materials and Methods).

### Biological inspection

The kidney represents the major target organ of heavy metal intoxication (Joshi *et al.*, 2017). Mercury ions which interact with the nucleophilic site of cellular or subcellular targets can readily and tightly bind to sulfur, such as cell groups of amino acids, proteins, and peptides, especially in the renal cortex and proximal tubule, through sodium ion channels which carry a mercury ion into renal tubule cells causing nephrotoxicity (Almeer *et al.*, 2019). Treatment strategies have mostly been directed at correcting circulatory disorders of the toxic effects of metals.

The results in Figures 1 and 2 show the effect of different treatment compounds on Aspartate aminotransferase (AST)/glutamic oxaloacetic transaminase (GOT), Alanine aminotransferase (ALT)/glutamic pyruvic transaminase (GPT), and alkaline phosphatase (ALP) activities in the serum  $\text{HgCl}_2$ -intoxicated group. A significant raise ( $p > 0.05$ ) was recorded in GOT, GPT, and ALP activities following  $\text{HgCl}_2$ -intoxication comparison with the control group.

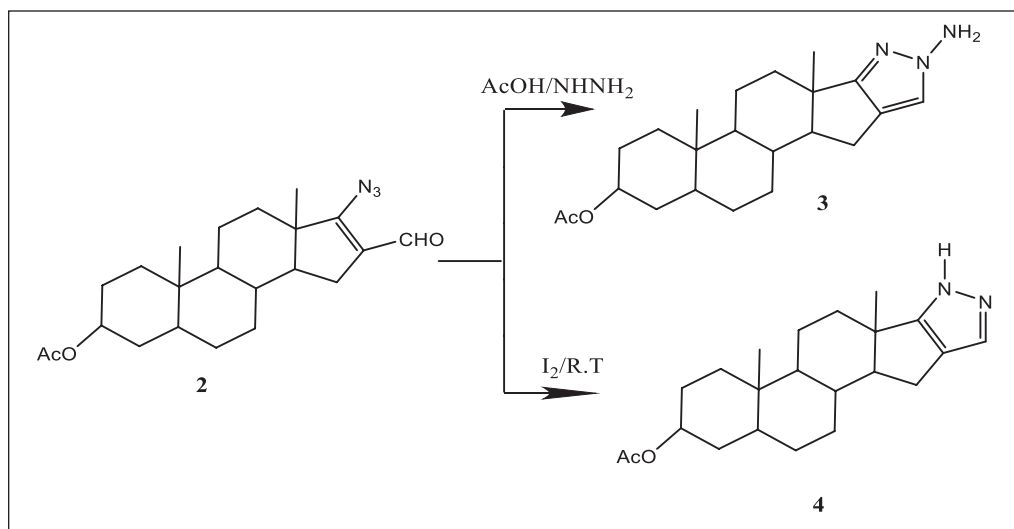
The activity of serum GPT and GOT in this study enhanced by  $\text{HgCl}_2$  treatment is in conformity with the study by El-Shenawy and Hassan (2008). This rise in enzymes is related to hepatocyte necrosis, and this leads to the release of these enzymes into the bloodstream (Sharma *et al.*, 2007). Also, the outcome of this research was in agreement with Abarikwu *et al.* (2017) who observed that during experimental Hg intoxication increased production of free radicals and oxidative stress, raised serum activities of GPT, GOT, ALP, and Lactate dehydrogenase (LDH), and lipid peroxidation (LPO) were reported.

These enzymes reduced significantly ( $p > 0.05$ ) in all tested compounds **4-**, **5-**, **6-**, and **9-**treated groups in comparison to the  $\text{HgCl}_2$  group (Figs. 1 and 2). Our results are consistent with those reported by Dragan *et al.* (2020); namely, the liver enzymes concentration values, treated with azetidin-2-one derivatives (compound **9**), were close to those recorded for losartan and slightly higher compared to the values for the healthy control group. In addition, Orabi *et al.* (2018) reported that pyrazole derivatives (compounds **4**, **5**, and **6**) have a powerful antioxidant activity and prevent cellular damage by prohibiting or quenching free radical reactions. Paudel *et al.* (2017) recorded that the elevated levels of liver functions such as GPT and GOT were attenuated by the administration of thiazole derivative (compound **6**) and this is in harmony with our results.

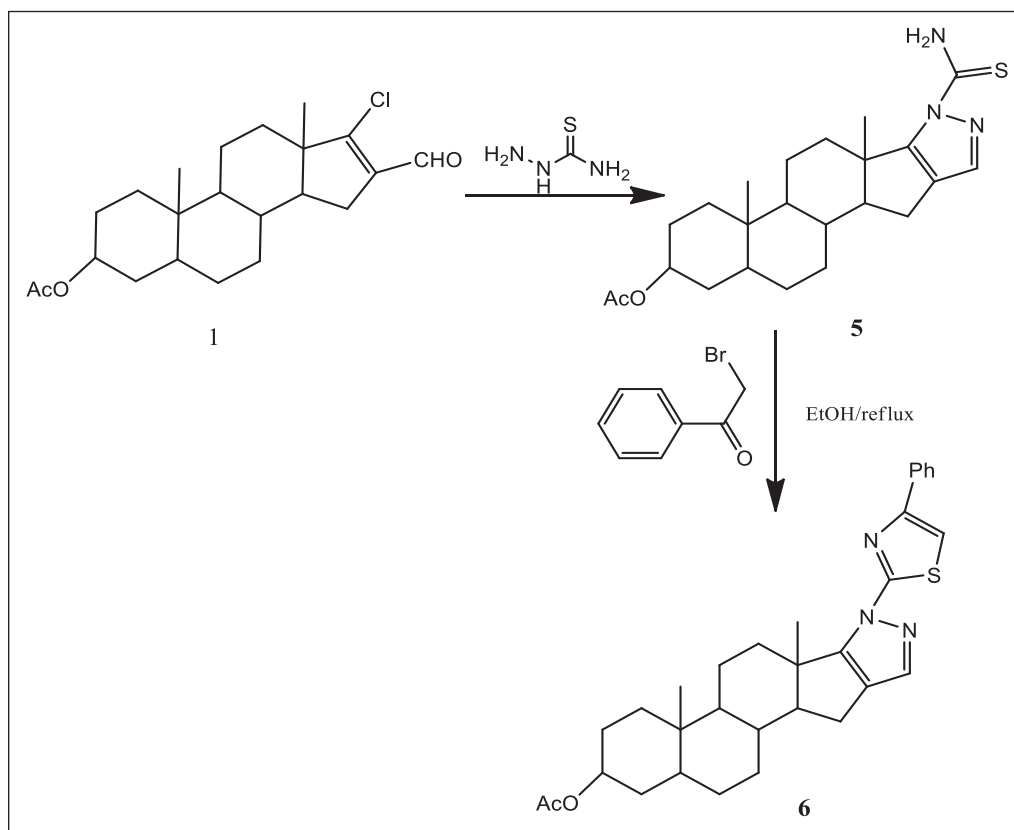
Rats bearing hepatocellular carcinoma treated with compounds **4**, **5**, and **6** (pyrazole derivative) showed remarkable diminishing in serum GPT, GOT, and ALP enzymes activity as well as urea and creatinine serum levels, which comes in line with El-Kady *et al.* (2019) and Shabbir *et al.* (2016) who listed meager change in serum values of GPT, GOT, and ALP in pyrazole compound-treated rats.

Moreover, a worthy depletion ( $p > 0.05$ ) in GPT, GOT, and ALP serum activities were detected in rats treated with losartan in comparison to the  $\text{HgCl}_2$ -intoxicated group (Figs. 1 and 2). Losartan is an efficient non-peptide blocker of angiotensin II receptors presented for clinical use in hypertension; it has the ability to scavenge the superoxide free radicals and increase the antioxidants through its prevention of free radical production (Ripley and Hirsch, 2010).

The data in Figure 3 illustrated the effect of different treatment compounds on serum lipid profiles that corroborate the findings of Merzoug *et al.* (2009). In this study,  $\text{HgCl}_2$ -induced causes an increase in the serum cholesterol, triglyceride, and low-density lipoprotein (LDL) was linked to hyperglycemia, with a concomitant decrease in serum high-density lipoprotein (HDL) ( $p > 0.05$ ) as compared to control one. Uzunhisarcikli *et al.* (2016) recorded that exposure to  $\text{HgCl}_2$  causes the leakage of glucose, triglycerides (TG), cholesterol, proteins, and LDL enzymes from the liver cytosol into the bloodstream and/or liver dysfunction and problems in the biosynthesis of these enzymes with altered hepatocyte membrane permeability which affects and increases the plasma levels of enzyme activities.



**Scheme 2.** Compound 2 yielded the pyrazoloandrostande derivatives 3 and 4.

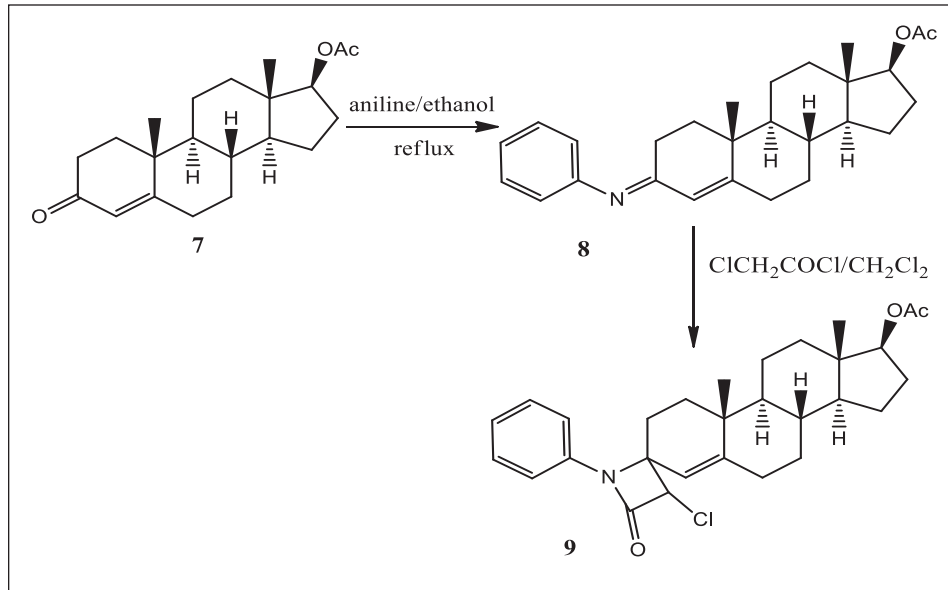


**Scheme 3.** Compound 1 yielded the pyrazoloandrostande derivatives 5 and 6.

In comparison to  $\text{HgCl}_2$ -intoxicated rats, all groups treated with tested compounds showed normal serum cholesterol, triglyceride, LDL, and HDL levels (**4**, **5**, **6**, and **9**) (Fig. 3). Our results are consistent with that of Fisher *et al.* (1991) who recorded that the steroidal heterocyclic compounds are powerful inhibitors of free radical output by excited monocytes and vigorous scavengers of lipid peroxyl radicals. It has been informed that

the anti-cholesterolemic effects of azetidin-2-ones (compound **9**) were observed by reclamation of the normal serum cholesterol and TG levels (Abeed *et al.*, 2017). So, these compounds are able to prevent LDL from oxidation as well as a reduction of cholesterol accumulation (Elmegeed *et al.*, 2005).

Also, losartan administration restored normal cholesterol, triglyceride, LDL, and HDL levels. This is possibly



**Scheme 4.** Ketone 7 yielded steroidal imine derivative 8 and was used as the starting material to synthesize the steroid spiroazitinone 9.

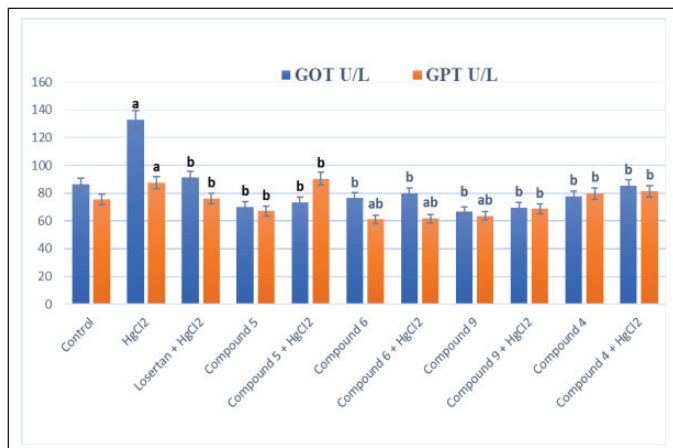


**Figure 1.** Effect of different treatment compounds on serum GPT and GOT activities in HgCl<sub>2</sub>-intoxicated rat groups. (a) Compared to control untreated group. (b) Compared to HgCl<sub>2</sub> group.

due to its hypolipidemic activities mechanism (Bhalerao and Kothari, 2018).

Figure 4 revealed the effect of different treatment compounds on homogenate urea and creatinine levels in the HgCl<sub>2</sub>-intoxicated rat group. Clinically, it is well established that serum creatinine and urea levels are indicators of renal function. A remarkable rise ( $p > 0.05$ ) in serum urea and creatinine levels was stated in the rats subjected to HgCl<sub>2</sub> in contrast to the normal group, reinforcing inorganic mercury as a nephrotoxic agent. Oxidative stress provoked by mercury which gives rise to urea augmentation could come from protein catabolism acceleration. The dwindling of protein content may be due to the declination and utilization of the degraded products for metabolic purposes (Ismail *et al.*, 2014). Also, our findings come in line with the study reported by Nava *et al.* (2000).

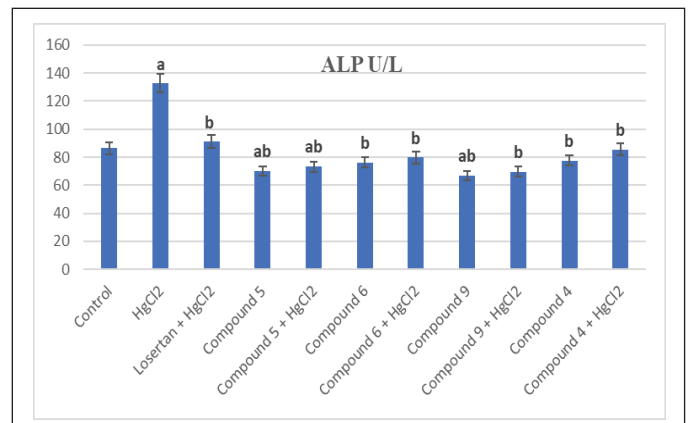


**Figure 2.** Effect of different treatment compounds on serum ALP activity in HgCl<sub>2</sub>-intoxicated rat groups. (a) Compared to control untreated group. (b) Compared to HgCl<sub>2</sub> group.

HgCl<sub>2</sub> toxicity mechanism is correlated with its effect on renal antioxidants; cellular oxidative stress led to stimulating HgCl<sub>2</sub> cellular toxicity, hence the creation of free radicals, LPO, and the elimination and destruction of impaired cellular glutathione peroxidase, Superoxide Dismutase (SOD), catalase (CAT), and file groups, and direct damage to DNA (Boroushaki *et al.*, 2014). Moreover, mercury join in this (small molecular weight protein) and metallothioneins inside the kidney; these interactions are thought to perform kidney toxicity leading to oxidative damage and cellular dysfunction owing to the overproduction of ROS in the kidney (Caglayan *et al.*, 2019).

Furthermore, a significant elevation of renal nitric oxide (NO) content was detected following HgCl<sub>2</sub> in comparison with the control group (Fig. 5). In addition, the renal level of malondialdehyde (MDA) was significantly increased in the HgCl<sub>2</sub>-treated group compared to the values obtained in the control and

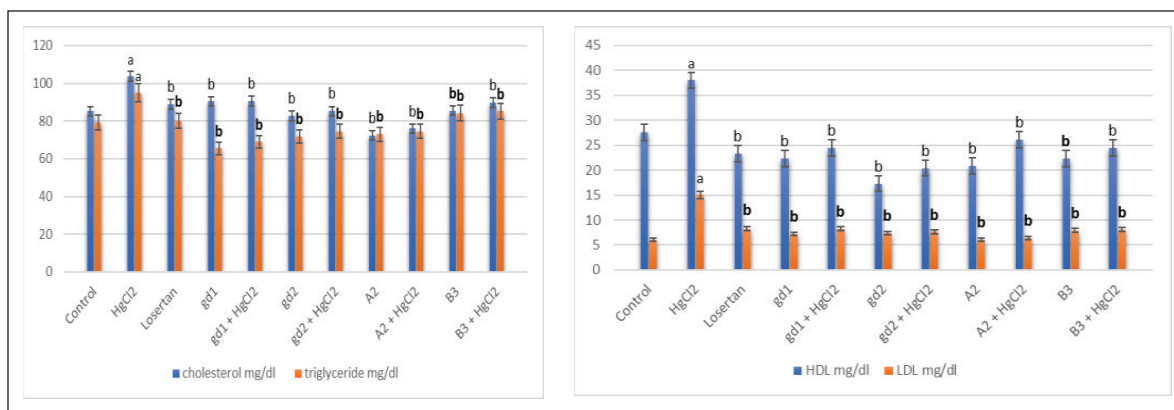


**Figure 3.** Effect of different treatment compounds on (lipid profiles) serum cholesterol, triglyceride, LDL, and HDL levels in HgCl<sub>2</sub>-intoxicated rats group. (a) Compared to control untreated group. (b) Compared to HgCl<sub>2</sub> group.

other groups (Fig. 6). Otherwise, renal CAT content was critically minimized following HgCl<sub>2</sub> intoxication (Fig. 7).

Our survey proved that group treatment with HgCl<sub>2</sub> significantly augments the MDA level, which is in concurrence with the former report of Agarwal *et al.* (2010). According to other studies, HgCl<sub>2</sub> enhances ROS as H<sub>2</sub>O<sub>2</sub> and superoxide, which trigger LPO and consequently oxidative tissue damage (Hosseini *et al.*, 2018). Karapehliyan *et al.* (2014) announced that acute treatment with a mercury-induced obvious increase in ROS, leading to LPO and protein degradation, finally led to cell death, and are associated with a decrease in cellular antioxidants and they elevate MDA level.

CAT enzyme is accountable for balancing between H<sub>2</sub>O<sub>2</sub> and superoxide radicals. Decreasing of CAT activity in this study because of exaggerated offspring hydroxyl ions and enhanced levels of hydroxyl radical also stimulate the rise of LPO levels in kidney and liver regions (Joshi *et al.*, 2014).

Our findings are in fulfillment of a study by Zhang *et al.* (2017) that confirmed that the CAT enzyme level was decreased on account of reduced regulation of expression; mRNA of Glutathione Peroxidase (GPx), SOD, and CAT were registered in the renal tissue. HgCl<sub>2</sub> intoxication has been answerable for the production of ROS and peroxide radicals, which further enhanced membrane LPO; also recovering NO in renal tissue might inasmuch the augmentation of iNOS. Formation of peroxynitrite (ONOO<sup>-</sup>) by much production of NO utilizes a cytotoxic function, which then passes the cell membrane, causes cellular molecule oxidation, interrupts the function of mitochondrial, increases caspase production, and leads to cell death (Ferrer-Sueta and Radi, 2009).

On the other hand, the administration of all tested compounds significantly induced depletion in serum urea (5, 6, 9, and 6) and creatinine (9, 6, 5, and 4) levels (Fig. 4).

Our findings are in agreement with the previous study of El-Kady *et al.* (2019) and Shabbir *et al.* (2016) who concluded with minor modulation in homogenate creatinine and urea values in rats treated with presale as compared with the controls. This datum affirmed the absence of nephrotoxicity or hepatotoxicity concerning the pyrazole derivative. Also, noteworthy exhaustion in the activity of serum GPT, GOT, and ALP enzymes is accompanied by the considerable consumption of homogenate urea and creatinine levels that are administered with thiazine derivative in agreement with Shabbir *et al.* (2016) who revealed

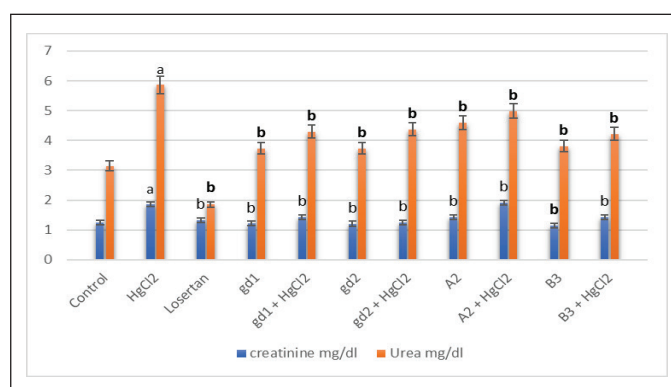


**Figure 4.** The effect of different treatment compounds on homogenate urea and creatinine levels in HgCl<sub>2</sub>-intoxicated rat group. (a) Compared to control untreated group. (b) Compared to HgCl<sub>2</sub> group.

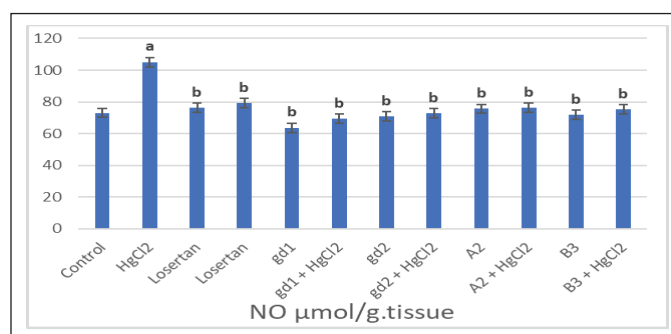


**Figure 5.** The effect of different treatment compounds on homogenate NO level in HgCl<sub>2</sub>-intoxicated rat group. (a) Compared to control untreated group. (b) Compared to HgCl<sub>2</sub> group.

a dropping in the activity of serum liver enzymes in animals remedied with thiazine derivatives; thus thiazine derivatives do not produce any signs of nephrotoxicity or hepatotoxicity. Likewise, the treatment of rats with all tested compounds (9, 6, 5, and 4) significantly retrieved the altered level of NO (Fig. 5). Also, all tested compounds (6, 5, 9, and 4) significantly decreased the MDA in renal tissues and succeed in restoring it to normal values (Fig. 6). Recuperation of normal renal CAT content was detected in all groups treated with tested compounds (5, 6, 9, and 4) and is

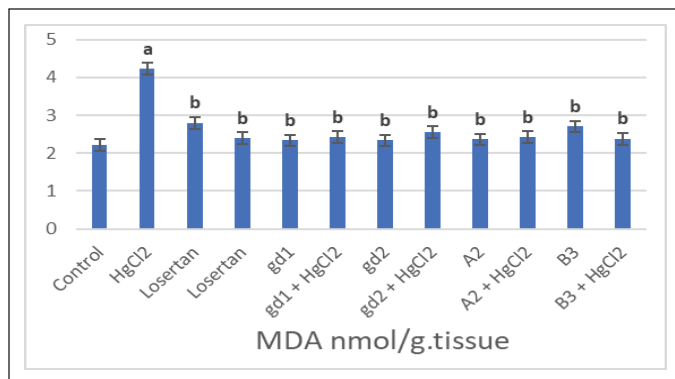


**Figure 6.** The effect of different treatment compounds on homogenate MDA level in HgCl<sub>2</sub>-intoxicated rat group.

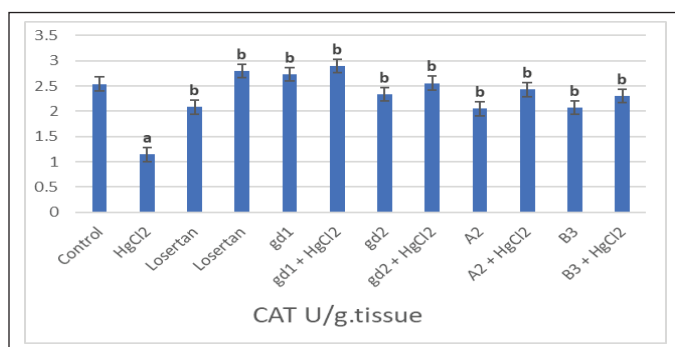


**Figure 7.** The effect of different treatment compounds on homogenate CAT level in HgCl<sub>2</sub>-intoxicated rat group. (a) Compared to control untreated group. (b) Compared to HgCl<sub>2</sub> group.

able to quench the HgCl<sub>2</sub>-induced reduction of renal CAT content (Fig. 7). These results concur with Asif (2018) who tested the free radical scavenging activities of azetidinone derivatives (compound 9) for their antioxidant activity. The derivatives with the chlorine substituent exhibited maximum activity and some azetidine derivatives used as the syntax for distinct, biologically active compounds, such as cholesterol absorption inhibitors and enzyme inhibitors, have been studied. A serious pathway of antioxidant agents is the inhibition of LPO that comes as an outcome of the interactivity between molecular oxygen and polyunsaturated fatty acids. These free radicals can oxidize biomolecules (e.g., lipids, proteins, and DNA) resulting in cell injury and death. In the liver, oral administration of pyrazole derivatives (compounds 4, 5, and 6) indicated that they could reinforce the antioxidant status. The increase in intracellular thiol-based antioxidant Glutathione (GSH) and the decreased MDA concentration were shown by compounds (Ali *et al.*, 2020). Palma-Vargas *et al.* (1996) postulated that after total liver ischemia, steroidal heterocyclic compounds remarkably enhance liver functions, via obstructing neutrophil permeation which is autonomous on nitrite/nitrate levels.

According to our results, losartan treatment produced a significant decrease in both homogenate urea and creatinine levels in comparison with the HgCl<sub>2</sub>-subjected group (Fig. 4). A significant depletion in renal NO content (Fig. 5) and MDA (Fig. 6) was observed in rats treated with losartan. Otherwise, treatment of rats with losartan restored renal CAT contents

more significantly than the HgCl<sub>2</sub> groups (Fig. 7). Losartan due to its antioxidant property may introduce its beneficial effects on antioxidant activities, restoration of NO bioavailability, and endothelial function (Kiran *et al.*, 2010; Trejo *et al.*, 2017).

Inflammation is the most important result of Hg-induced renal toxicity, as shown in Figure 8, in comparison to the control group overproduction of tumor necrosis factor-alpha (TNF- $\alpha$ ) and interleukin-1 (IL-1) by Hg intoxication triggered proinflammatory signaling. It has been suggested that mercury treats manifest significant renal tubular toxicity, leading to the release of self-antigen and the development of inflammatory repayment, cytokines, and autoantibody manufacturing (Pollard *et al.*, 2019). Also, Li *et al.* (2010) announced that Hg aggregation in renal tissue causes body weight lost and increased antioxidant markers like urea, creatinine, Kim-1 expression, NO offspring and LPO, repression of the Nrf2-antioxidant restraint path, upregulation of IL-1 $\beta$ , TNF- $\alpha$ , and potentiation of proapoptotic activity; hence, Hg improver ROS production as well led to animated nuclear factor kappa B and overexpression of proinflammatory cytokines (Almeer *et al.*, 2019). It is interesting that mercury spurs the expression of mRNA TNF- $\alpha$  and IL-6 and activated p38 mitogen-activated protein kinase (p38 MAPK). So, mercury activated p38 MAPK by inhibiting the NF-kappa B pathway and adjusting cytokine expression (Kim *et al.*, 2002).

On the other hand, tested compound treatment is accompanied by a remarkable inhibition of TNF- $\alpha$  and IL-1  $\beta$  serum levels in comparison with groups administered HgCl<sub>2</sub> only. The antioxidant activity of isoxazoline and parasailing may be due to their potent radical-scavenging and anti-inflammatory activity which is enhanced by increasing the aromaticity of the substituted group also. Azetidinone derivatives have been identified as Transarterial chemoembolization (TACE) inhibitors with novel biological activities, such as anticancer, cardiovascular, and anti-inflammatory activities (Zakia *et al.*, 2006). Also, Sadrzadeh and Naji (1998) announced the ability of aminosteroids to reduce levels of proinflammatory stimuli such as LPO, TNF- $\alpha$ , and cyclooxygenase-2.

Furthermore, losartan treatment produced observed diminishing ( $p > 0.05$ ) in serum TNF- $\alpha$  and IL-1  $\beta$  levels in comparison with the HgCl<sub>2</sub>-intoxicated group (Fig. 8). Treatment with losartan reduced neutrophil mobilization, hyper nociception, and IL-1 $\beta$  and TNF- $\alpha$  production (Silveira *et al.*, 2013).

Concerning the effect of different treatment compounds on Nephren-2 and KIM-1 gene expression levels in the HgCl<sub>2</sub>-intoxicated rats group (Fig. 9), it was manifested that, in contrast with the control group, rats treated with HgCl<sub>2</sub> produced a significant upregulation in KIM-1 and Nephren-2 gene expression levels. It has been reported that mercury compounds cause DNA breakage via free radical reactions that may attack DNA integrity and accelerate the apoptosis process of germ cells (Boujbiha *et al.*, 2009). Mercury pool in renal tissue has been associated with impaired renal function, by increased expression of Kim-1 mRNA. Protein and KIM-1 mRNA are expressed at a low level in healthy kidneys, but significantly increased levels in post-ischemic kidneys. These high renal indices are due to damage to the renal tubules after exposure to mercury (Almeer *et al.*, 2019). Furthermore, HgCl<sub>2</sub> assembles in lysosomes and inhibits the average of adenosine 5'-triphosphate (ATP) synthesis in

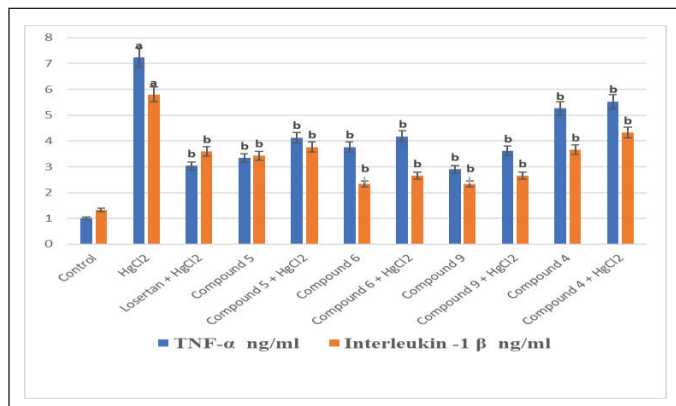


**Figure 8.** Effect of different treatment compounds on serum TNF- $\alpha$  (inflammatory biomarker) and IL-1  $\beta$  levels in HgCl<sub>2</sub>-intoxicated rat group. (a) Compared to control untreated group. (b) Compared to HgCl<sub>2</sub> group.

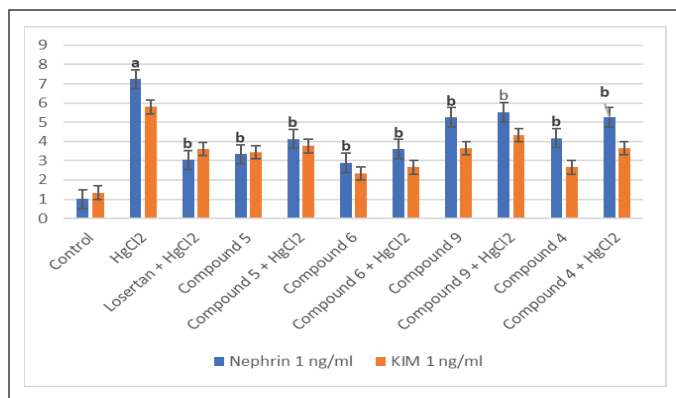


**Figure 9.** Effect of different treatment compounds at nephtrin-2 and KIM-1 gene expression levels in HgCl<sub>2</sub>-intoxicated rat group. (a) Compared to control untreated group. (b) Compared to HgCl<sub>2</sub> group.

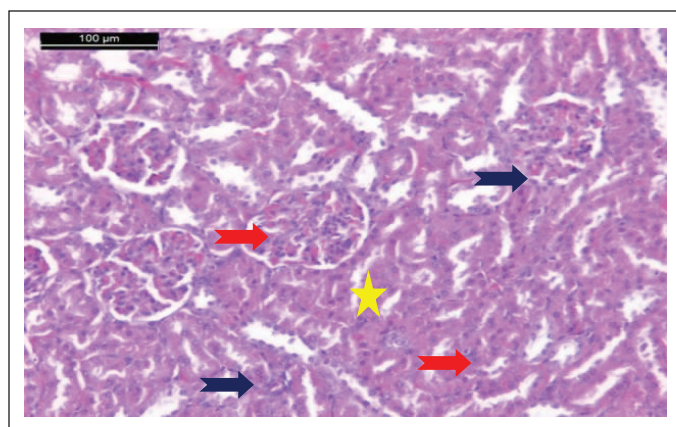


**Figure 10.** Photomicrograph of kidney of control healthy group showing that a typical glomerulus and Bowman’s capsule are intact with simple cuboidal epithelial lining. It also exhibited that the proximal tubule (blue arrow) and distal convoluted tubule (red arrow) are normal (H & E stain, Scale bar 100  $\mu$ m).

mitochondria. It was found that HgCl<sub>2</sub>-induced more rapid drops in neoprene mRNA (Luimula *et al.*, 2000a).

On the other hand, the tested compounds (6, 5, 4, and 9) treatment was accompanied by a significant downregulation

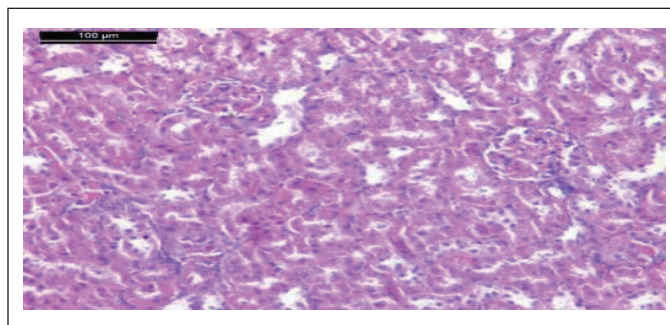


**Figure 11.** Photomicrograph of kidney of HgCl<sub>2</sub> group showing mild interstitial congestion, focal interstitial hemorrhage, severe tubular necrosis, atrophy of renal tissue, and inflammatory infiltration (H & E stain, Scale bar 100  $\mu$ m).

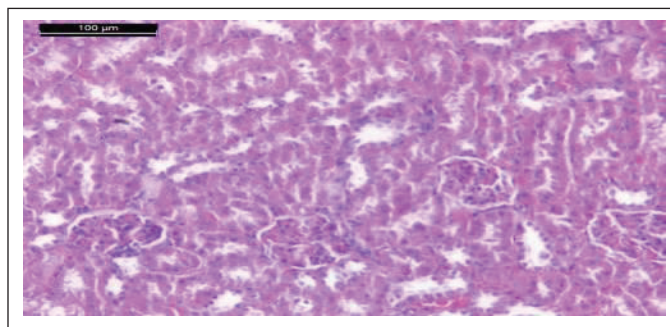


**Figure 12.** Photomicrograph of kidney of rat treated with losartan and HgCl<sub>2</sub> group showing tubular dilatation, lack of nuclei, and diffuse degeneration and necrosis in the proximal tubular (H & E stain, Scale bar 100  $\mu$ m).

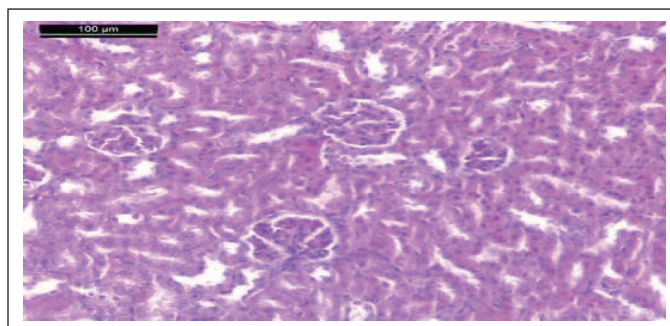


**Figure 13.** Photomicrograph of kidney of comp. 5 given rat showing normal glomeruli and renal tubules (H & E stain, Scale bar 100  $\mu$ m).

in KIM-1 and Nephtrin-2 gene expression levels in comparison with groups administered HgCl<sub>2</sub> only. KIM-1 is an epithelial cell adhesion molecule regulated in cells, and it is detached and undergoes replication, and KIM-1 has an important role in restoring morphological integrity and renal function after ischemia (Ichimura *et al.*, 1998). Neoprene plays roles in cell-cell adhesion and/or signal transduction and is an unprecedented transmembrane protein of renal glomerular podocytes, which appears to be extremely important for maintaining the glomerular filtration barrier (Luimula *et al.*, 2000b).

In addition, the expression of KIM-1 and Nephtrin-2 gene expression levels near to control group in comparison with the HgCl<sub>2</sub> treated group were decreased with losartan (Fig. 9). This may have resulted from hypotension at the glomerular filtration

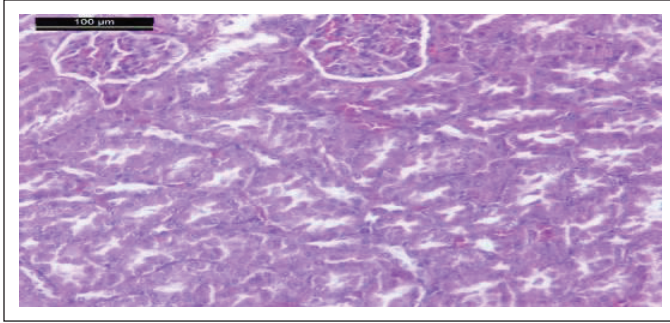


**Figure 14.** Photomicrograph of kidney of HgCl<sub>2</sub> + **comp. 5** given rat showing normal glomeruli and renal tubules (H & E stain, Scale bar 100 μm).

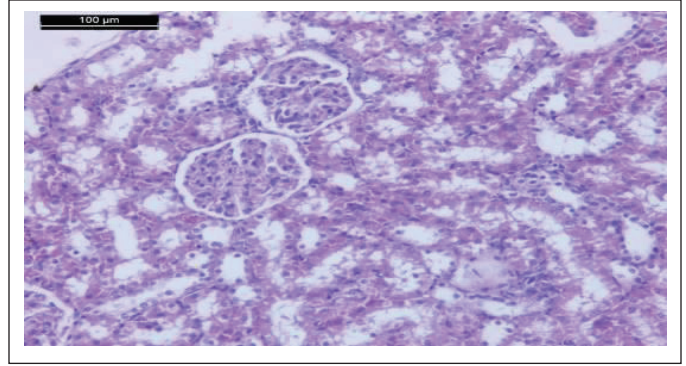


**Figure 16.** Photomicrograph of kidney of HgCl<sub>2</sub> + **comp. 9** given rat showing normal glomeruli and renal tubules (H & E stain, Scale bar 100 μm).

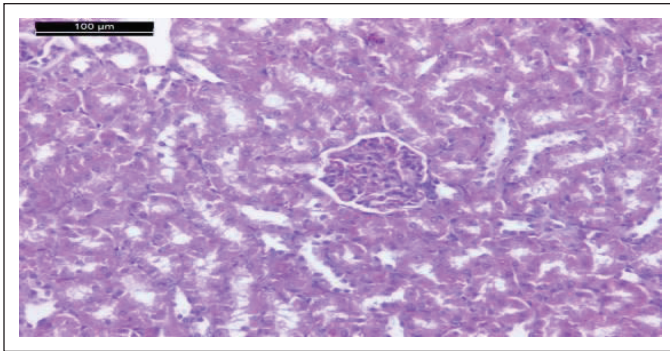


**Figure 15.** Photomicrograph of kidney of **comp. 9** given rat showing normal glomeruli and renal tubules (H & E stain, Scale bar 100 μm).

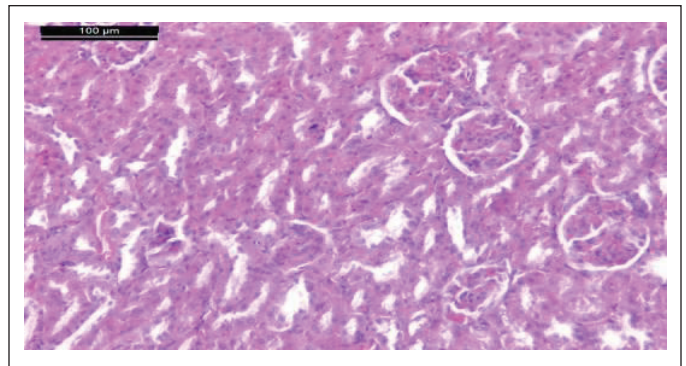


**Figure 17.** Photomicrograph of kidney of rat given **comp. 6** showing different damage of glomeruli. These alterations are in the form of a trophy, lobulated, and hypercellularity (H & E stain, Scale bar 100 μm).

barrier that decreased neoprene content, finally contributing to the improvement of renal function (Trejo *et al.*, 2017).

### Histopathology results

Microscopic examinations of renal tissue of the control group showed that typical glomerulus and Bowman's capsule are intact with simple cuboidal epithelial lining. The proximal tubule and distal convoluted tubule are also normal (Fig. 10). HgCl<sub>2</sub> has a vigorous nephrotoxic effect. Inside the kidney, the majority of Hg<sup>2+</sup> remains in plasma after exposure to HgCl<sub>2</sub>, and sulfhydryl-containing ligands as glutathione (GSH) and albumin react with it to form the Hg<sup>2+</sup>-GSH complex in the glomeruli and in the proximal tubules it degrades to Hg<sup>2+</sup>-cysteine by the combined action of gamma-glutamyl transpeptidase and dipeptidase found in epithelial cells. The resulting product is then aggregated and assembled into the epithelial cells of the proximal tubules. Finally, it produces inflammation and acute tubular necrosis (ATN) through the cytotoxic effect of Hg<sup>2+</sup> accumulated in epithelial cells (Yanagisawa, 1998).

Microscopic investigations of the kidney of the HgCl<sub>2</sub> group showed mild interstitial congestion, focal interstitial hemorrhage, severe tubular necrosis, and atrophy of renal tissue inflammatory infiltration was also seen (Fig. 11). The normal renal corpuscle's histological structure and renal tubules are shown in the kidney tissue control rat group, while photomicrograph of the kidney of the HgCl<sub>2</sub> group showed mild interstitial congestion, focal interstitial hemorrhage, severe tubular necrosis, atrophy of renal tissue, and inflammatory infiltration. The reaction of

mercury with sulfhydryl protein groups is supposed to be the one that plays a cellular-level substantial role in mercury-induced nephrotoxicity. Alteration in mitochondrial morphology and function is an extremely early event following the administration of HgCl<sub>2</sub> (Hanif *et al.*, 2022). Yanagisawa (1998) and Al-Zubaidi and Rabee (2015) suggested that mitochondrial dysfunction and oxidative damage have proposed a major role in mercury pathogenic mechanisms which induced renal toxicity. A forceful nephrotoxic agent of HgCl<sub>2</sub> inspires nephritic syndrome, immunologic glomerulonephritis, or ATN. Several research works have recalled the mechanism of HgCl<sub>2</sub>-induced kidney injury through the depletion of cellular cysteine thiols that increase oxidative stress and rebate antioxidant enzyme activity, lessening ATP content (Caglayan *et al.*, 2019). Inflammation and apoptosis, besides, disturb and eliminate several physiological and regulatory functions as a result of mercury binding with essential elements such as zinc and selenium (Fiuza *et al.*, 2018).

Moreover, histological examination of the kidneys of losartan and HgCl<sub>2</sub>-treated rats showed tubular dilatation, nucleolar loss, extensive proliferation, and proximal tubule necrosis (Fig. 12).

Photomicrograph of kidneys of compounds (5, 9, 6, and 4) rat group showed normal glomeruli and renal tubules as the control group (Figs. 13, 15, 17, and 19). Owing to anti-inflammatory, antitubercular, antioxidant, and cardiovascular activities (Asif,

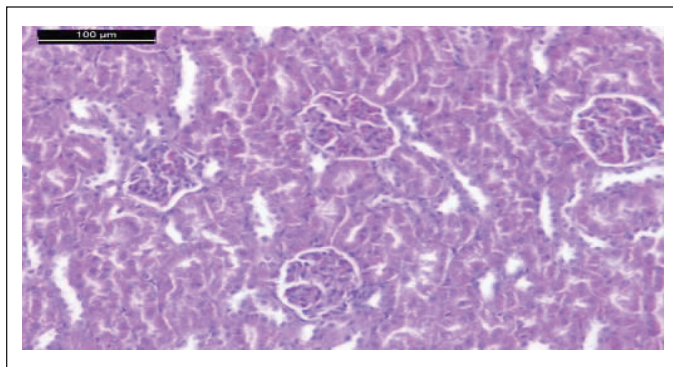


**Figure 18.** Photomicrograph of kidney of rat given HgCl<sub>2</sub> + **comp. 6** showing the glomeruli and renal tubules more or less like normal (H & E stain, Scale bar 100 μm).

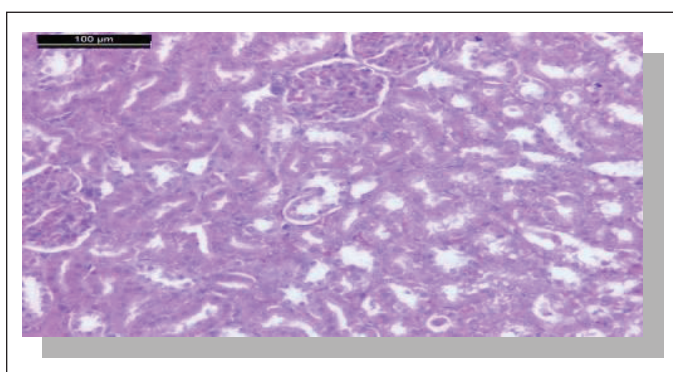


**Figure 19.** Photomicrograph of kidney of rat given **comp. 4** only showing normal glomeruli and renal tubules. Notice the presence of some degenerative tubules (H & E stain, Scale bar 100 μm).

2018), as inhibitors of protein glycation (Karrouchi *et al.*, 2018), treatment with all our synthetic compounds offers an important defense from HgCl<sub>2</sub>-induced acute renal failure (Figs. 14, 16, 18, and 20). According to our findings, we suggested that the presence of the pyrazole ring which has important pharmacological and therapeutic properties is able to restore the changes produced by HgCl<sub>2</sub> intoxication.

## CONCLUSION

In conclusion, a series of new heterocyclic steroidal derivatives have been modified and structurally confirmed. Modification of steroid moiety with heterocyclic rings displayed valuable biological activities and could be acting as a beneficial treatment for the amelioration of renal injury induced by HgCl<sub>2</sub>. According to our results, we can conclude that, the biological profiles of these new generations of heterocyclic steroid derivatives presented by their antioxidant and anti-inflammatory properties would be considered as a fruitful matrix for the further development of promising medicinal agents.

## AUTHORS' CONTRIBUTIONS

S. H. M., N. A., and D.S.E. wrote the original draft of the manuscript. S. H. M. and N. A. A. revised the manuscript. G. A. E. and D. S. E. performed the chemical section. S. H. M., N. A.

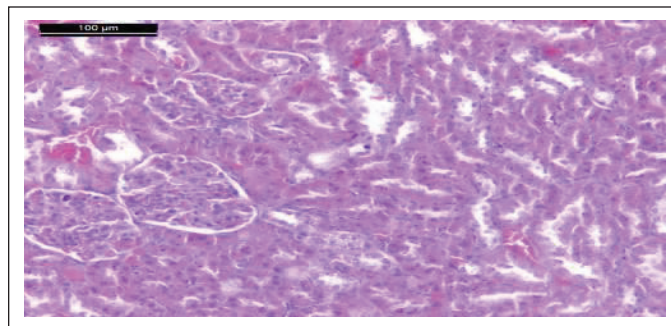


**Figure 20.** Photomicrograph of kidney of rat given HgCl<sub>2</sub> + **comp. 4** showing the glomeruli and renal tubules like normal features (H & E stain, Scale bar 100 μm).

**Table 1.** Primer sequences for RT-PCR.

Ref.	Primer sequence (5'-3')	Gene
(Prozialeck <i>et al.</i> , 2009)	F: TGGCACTGTGACATCCTCAGA R: GCAACGGACATGCCAACATA	KIM-1
(Ma <i>et al.</i> , 2013)	F: TGCTGAAGGCGAGGACAT R: TGTAGGAAACGGGTGTTGTGAAG	Nephrin
(Prozialeck <i>et al.</i> , 2009)	F: CCTGGAGAAACCTGC-CAAGTAT R: AGCCAGGATGCCCTTAGT	GAPDH

F: forward primer; R: reverse primer.

A., and M. I. E. performed the experiments and analyzed the data. A-R. H. F. performed the pathology section.

## FINANCIAL SUPPORT

There is no funding to report.

## CONFLICTS OF INTEREST

The authors declare that they have no known financial conflicts of interest or personal relationships that could appear to influence the work reported in this article.

## ETHICAL APPROVAL

This article does not contain any studies with human participants or animals performed by any of the authors.

## DATA AVAILABILITY

All data generated and analyzed are included in this research article.

## PUBLISHER'S NOTE

This journal remains neutral with regard to jurisdictional claims in published institutional affiliation.

## REFERENCES

- Abarikwu SO, Benjamin S, Ebah SG, Obilor G, Agbam G. Protective effect of *Moringa oleifera* oil against HgCl<sub>2</sub>-induced hepato- and nephro-toxicity in rats. *J Basic Clin Physiol Pharmacol*, 2017; 28(4):337-45; doi: 10.1515/jbcpp-2016-0033.
- Abeed A, Youssef M, Hegazy R. Synthesis, anti-diabetic and renoprotective activity of some new benzazole, thiazolidin-4-one and azetidin-2-one derivatives. *J Braz Chem Soc*, 2017; 28(11); doi: 10.21577/0103-5053.20170050.

- Aebi H. Catalase in vitro. *Methods Enzymol*, 1984; 105:121–6; doi: 10.1016/s0076-6879(84)05016-3.
- Agarwal R, Goel SK, Chandra R, Behari JR. Role of vitamin E in preventing acute mercury toxicity in rat. *Environ Toxicol Pharmacol*, 2010; 29:70–8; doi: 10.1016/j.etap.2009.10.003.
- Ali SA, Awad SM, Said AM, Mahgoub S, Taha H, Ahmed NM. Design, synthesis, molecular model and biological evaluation of novel 3-(2-naphthyl)-1-phenyl-1H-pyrazole derivatives as potent antioxidants and 15-Lipoxygenase inhibitors. *J Enzyme Inhib Med Chem*, 2020; 35(1):847–63; doi: 10.1080/14756366.2020.1742116.
- Almeer RS, Albasher G, Alotibi F, Alarifi S, Ali D, Alkahtani S. *Ziziphus spina-christi* Leaf extract suppressed mercury chloride-induced nephrotoxicity via Nrf2-antioxidant pathway activation and inhibition of inflammatory and apoptotic signaling. *Oxid Med Cell Longev*, 2019; 2019:5634685; doi: 10.1155/2019/5634685.
- Al-Zubaidi ES, Rabee AM. Effect of mercuric chloride on biochemical and hematological parameters in male albino mice. *International Journal of Science and Research* 2015; 6:6–391; doi: 10.21275/ART20173105.
- Armitage P, Berry G. Comparison of several groups: statistical method in medical research. 2nd edition, Blackwell Significant Publication, Oxford, UK, pp 186–213, 1987.
- Asif M. Antimicrobial potential of various substituted azetidine derivatives. *MOJ Biorg Org Chem*, 2018; 2(2):36–40; doi: 10.15406/mojboc.2018.02.00053.
- Balali-Mood M, Naseri K, Tahergorabi Z, Khazdair MR, Sadeghi M. Toxic mechanisms of five heavy metals: mercury, lead, chromium, cadmium, and Arsenic. *Front Pharmacol*, 2021; <https://doi.org/10.3389/fphar.2021.643972>.
- Belfield DM. Goldberg, colorimetric method for determination of alkaline phosphatase. *Enzyme*, 1971; 12(5):561–8.
- Berkels R, Purol-Schnabel S, Rösen R. Measurement of nitric oxide by reversion of nitrate/nitrite to no. *Methods Mol Biol*, 2004; 279:1–8; doi:10.1385/1-59259-807-2.001.
- Bhalerao MK, Kothari S. Effect of cilnidipine versus losartan on lipid profile in patients of hypertension with or without diabetes. *Indian J Appl Res*, 2018; 8(5); doi: 10.36106/ijar.
- Borouhaki MT, Mollazadeh H, Rajabian A, Dolati K, Hoseini A, Paseban M, Farzadnia M. Protective effect of pomegranate seed oil against mercuric chloride-induced nephrotoxicity in rat. *Ren Fail*, 2014; 36(10):1581–6; doi: 10.3109/0886022X.2014.949770.
- Boujbiha MA, Hamden K, Guermazi F, Bouslama A, Omezzine A, Kammoun A, El Fekia A. Testicular toxicity in mercuric chloride treated rats: association with oxidative stress. *Reprod Toxicol*, 2009; 28:81–9; doi: 10.1016/j.reprotox.2009.03.011.
- Caglayan C, Kandemir FM, Yildirim S, Kucukler S, Eser G. Rutin protects mercuric chloride-induced nephrotoxicity via targeting of aquaporin 1 level, oxidative stress, apoptosis and inflammation in rats. *J Trace Elem Med Biol*, 2019; 54:69–78; doi: 10.1016/j.jtemb.2019.04.007.
- Dashbaldan S, Rogowska A, Pączkowski C, Szakiel A. Distribution of triterpenoids and steroids in developing *Rugosa* Rose (*Rosarugosa Thunb.*) accessory fruit. *Molecules*, 2021; 26:5158; <https://doi.org/10.3390/molecules26175158>.
- Dragan M, Stan CD, Iacob AT, Dragostin OM, Boanca M, Lupusoru CE, Zamfir CL, Profire L. Biological evaluation of azetidine-2-ones derivatives of ferulic acid as promising anti-inflammatory agents. *Processes*, 2020; 8:1401; doi:10.3390/pr8111401.
- Drury RAB, Wallington EA. 1980. Carleton's histological technique. 5th edition, Toronto: Oxford University Press, Oxford, NY, pp 188–89.
- El-Kady DS, Ali NA, Sayed AH, Abdelhalim MM, Elmegeed GA, Ahmed HH. Assessment of the antitumor potentiality of newly designed steroid derivatives: pre-clinical study. *Asian Pac J Cancer Prev*, 2019; 20(10):3057–70; doi: 10.31557/APJCP.2019.20.10.3057.
- Elmegeed GA. Synthesis of novel pyrazolo pyrimidino and pyrido androstane derivatives of pharmacological interest. *Egypt J Chem*, 2004; 47(6):579–89.
- Elmegeed GA, Ahmed H, Hussein JS. Novel synthesized aminosteroidal heterocycles intervention for inhibiting iron-induced oxidative stress. *Eur J Med Chem*, 2005; 40:1283–94; doi: 10.1016/j.ejmech.2005.07.012
- El-Shenawy SM, Hassan NS. Comparative evaluation of the protective effect of selenium and garlic against liver and kidney damage induced by mercury chloride in the rats. *Pharmacol Rep*, 2008; 60(2):199–208.
- Ferrer-Sueta G, Radi R. Chemical biology of peroxynitrite: kinetics, diffusion, and radicals. *ACS Chem Biol*, 2009; 4(3):161–77; doi: 10.1021/cb800279q.
- Fisher PH, Levine EM, Doyle MM, Arpano MM, Hoogasian JJ. A 21-aminosteroid inhibits oxidation of human low density lipoprotein by human monocytes and copper. *Atherosclerosis*, 1991; 90:197–202.
- Fiuza T, Leitemperger J, Severo E, Marins A, Amaral A, Pereira M, Loro V. Effects of diphenyl diselenide diet on a model of mercury poisoning. *Mol Biol Repo*, 2018; 45(7); doi: 10.1007/s11033-018-4433-z.
- Fossati P, Prencipe L. Serum triglycerides determined colorimetrically with an enzyme that produces hydrogen peroxidase. *Clin Chem*, 1982; 28:2077–80.
- Fuente A, Reyes M, Alvarez YM, Ruiz JA, Vélez H, Viñas-Bravo O, Montiel-Smith S, Meza-Reyes S, Sandoval-Ramirez J. 1H and 13C NMR spectral assignment of androstane derivatives. *Magn Reson Chem*, 2005; 43(8):676–8; doi.org/10.1002/mrc.1605.
- González E, Gutiérrez E, Galeano C, Chevia C, de Sequera P, Bernis C, Parra EG, Delgado R, Sanz M, Ortiz M, Goicoechea M, Quereda C, Olea T, Bouarich H, Hernández Y, Segovia B, Praga M. Early steroid treatment improves the recovery of renal function in patients with drug-induced acute interstitial nephritis. *Kidney Int*, 2008; 73(8):940–6; doi:10.1038/sj.ki.5002776.
- Hanif MO, Bali A, Ramphul K. Acute renal tubular necrosis. [Updated 2022 Jul 5]. In: StatPearls [Internet]. StatPearls Publishing, Treasure Island, FL. Available via <https://www.ncbi.nlm.nih.gov/books/NBK507815>.
- Henry TJ. 1974. Clinical chemistry principles and techniques. 2th edition, Harper and Row Publishers, New York, NY.
- Hosseini A, Rajabian A, Fanoudi S, Farzadnia M, Borouhaki MT. Protective effect of *Rheum turkestanicum* root against mercuric chloride-induced hepatorenal toxicity in rats. *Avicenna J Phytomed*, 2018; 8(6):488–97.
- Ichimura JV, Bonventre V, Bailly V, Wei H, Hession CA, Cate RL, Sanicola M. Kidney injury molecule-1 (KIM-1), a putative epithelial cell adhesion molecule containing a novel immunoglobulin domain, is up-regulated in renal cells after injury. *J Biol Chem*, 1998; 273(7):4135–42; doi: 10.1074/jbc.273.7.4135.
- Ismail SM, Ismail HA, Al-Sharif GM. Protective effect of L-ascorbic acid (Vitamin C) on mercury detoxication and physiological aspects of Albino rats. *Int J Med Health Sci Res, Conscientia Beam*, 2014; 1(11):126–32.
- Joshi D, Mittal DK, Shukla S, Srivastav AK, Srivastav SK. N-acetyl cysteine and selenium protects mercuric chloride-induced oxidative stress and antioxidant defense system in liver and kidney of rats: a histopathological approach. *J Trace Elem Med Biol*, 2014; 28:218–26.
- Joshi D, Srivastav SK, Belemkar S, Dixit VA. *Zingiber officinale* and 6-gingerol alleviate liver and kidney dysfunctions and oxidative stress induced by mercuric chloride in male rats: a protective approach. *Biomed Pharmacother*, 2017; 91:645–55; doi: 10.1016/j.biopha.2017.04.108.
- Karapehlihan M, Ögün M, Kaya I, Özen H, Deveci H, Karaman M. Protective effect of omega-3 fatty acid against mercury chloride intoxication in mice. *J Trace Elem Med Biol*, 2014; 28:94–9; doi: 10.1016/j.jtemb.2013.08.004.
- Karrouchi K, Radi S, Ramli Y, Taoufik J, Mabkhot YN, Al-Aizari FA, Ansar M. Synthesis and pharmacological activities of pyrazole derivatives: a review. *Molecules*, 2018; 23(1):134; <https://doi.org/10.3390/molecules23010134>.
- Kim SH, Johnson VJ, Sharma RP. Mercury inhibits nitric oxide production but activates proinflammatory cytokine expression in murine macrophage: differential modulation of NF-kappaB and p38 MAPK signaling pathways. *Nitric Oxide*, 2002; 7(1):67–74; doi: 10.1016/s1089-8603(02)00008-3. PMID: 12175822.

- Kiran VU, Rajaiah N, Devarakonda K, Reddy Y. Effect of losartan and ramipril on oxidative stress and anti-oxidant status in South Indian hypertensive patients. *Int J Pharmacol*, 2010; 6:916–20; doi: 10.3923/ijp.2010.916.920.
- Li S, Wang X, Xiao Y, Wang Y, Wan Y, Li X, Li Q, Tang X, Cai D, Ran B, Wu C. Curcumin ameliorates mercuric chloride-induced liver injury via modulating cytochrome P450 signaling and Nrf2/HO-1 pathway. *Ecotoxicol Environ Saf*, 2020; 208:111426; doi: 10.1016/j.ecoenv.2020.111426.
- Luimula P, Aaltonen P, Ahola H, Palmén T, Holthöfer H. Alternatively spliced nephrin in experimental glomerular disease of the rat. *Pediatr Res*, 2000b; 48:759–62; <https://doi.org/10.1203/00006450-200012000-00010>.
- Luimula P, Ahola H, Wang S, Solin P, Aaltonen, Tikkanen I, Kerjaschki D, Holthöfer H. Cell biology – immunology – pathology nephrin in experimental glomerular disease. *Kidney Int*, 2000a; 58(4):1461–8; doi: 10.1046/j.1523-1755.2000.00308.x.
- Ma R, Liu L, Liu X, Wang Y, Jiang W, Xu L. Triptolide markedly attenuates albuminuria and podocyte injury in an animal model of diabetic nephropathy. *Exp Ther Med*, 2013; 6:649–56; <https://doi.org/10.3892/etm.2013.1226>.
- Merzoug S, Toumi ML, Oumeddour A, Boukhris N, Baudin B, Tahraoui A, Bairi A. Effect of inorganic mercury on biochemical parameters in Wistar rat. *J Cell Anim Biol*, 2009; 3(12):222–30.
- Nava M, Romero F, Quiroz Y, Parra G, Bonet L, Rodríguez-Iturbe B. Melatonin attenuates acute renal failure and oxidative stress induced by mercuric chloride in rats. *Am J Physiol Renal Physiol*, 2000; 279(5):F910–8; doi: 10.1152/ajprenal.2000.279.5.F910.
- Orabi EA, Orabib MAA, Mahrossc MH, Abdel-Hakim M. Computational investigation of the structure and antioxidant activity of some pyrazole and pyrazolone derivatives. *J Saudi Chem Soc*, 2018; 22:705–14; <https://doi.org/10.1016/j.jscs.2017.12.003>.
- Palma-Vargas JM, Toledo AH, Garcia-Criado FJ, Misawa K, Lopez-Nebolina F, Toledo-Pereyra LH. 21-Aminosteroids block neutrophil infiltration and provide liver protection independent of NO<sub>2</sub>/NO<sub>3</sub>- levels. *J Surg Res*, 1996; 66:131–7; <https://doi.org/10.1006/jsre.1996.0384>.
- Patton CJ, Crouch SR. Spectrophotometric and kinetics investigation of the Berthelot reaction for the determination of ammonia. *Anal Chem*, 1977; 49(3):464–9; <https://doi.org/10.1021/ac50011a034>.
- Paudel SO, Benjamin S, Ebah SG, Obilor G, Agbam G. Protective effect of *Moringa oleifera* oil against HgCl<sub>2</sub>-induced hepato- and nephro-toxicity in rats. *J Basic Clin Physiol Pharmacol*, 2017; 28(4):337–45; doi: 10.1515/jbcpp-2016-0033.
- Pollard MM, Cauvi DM, Toomey CB, Hultman P, Kono DH. Mercury-induced inflammation and autoimmunity. *Biochim Biophys Acta (BBA) Gen Subj*, 2019; 1863(12):129–299; doi: 10.1016/j.bbagen.2019.02.001.
- Prozialeck WC, Edwards JR, Lamar PC, Liu J, Vaidya VS, Bonventre JV. Expression of kidney injury molecule-1 (Kim-1) in relation to necrosis and apoptosis during the early stages of Cd-induced proximal tubule injury. *Toxicol Appl Pharmacol*, 2009; 238(3):306–14; <https://doi.org/10.1016/j.taap.2009.01.016>.
- Reitman S, Frankel S. A colorimetric method for the determination of serum glutamic oxaloacetic and glutamic pyruvic transaminase. *Am J Clin*, 1957; 28:56–63; doi: 10.1093/ajcp/28.1.56.
- Ripley E, Hirsch A. Fifteen years of losartan: what have we learned about losartan that can benefit chronic kidney disease patients? *Int J Nephrol Renovasc Dis*, 2010; 3:93–8; doi: 10.2147/ijnrd.s7038.
- Sadrzadeh SM, Naji AA. The 21-aminosteroid 16-desmethyl tirilazad mesylate prevents necroinflammatory changes in experimental alcoholic liver disease. *J Pharmacol Exp Ther*, 1998; 284:406–12.
- Salman MA, Kotb AM, Haridy MAM, Hammad S. Hepato- and nephroprotective effects of bradykinin potentiating factor from scorpion (*Buthus occitanus*) venom on mercuric chloride-treated rats. *EXCLI J*, 2016; 15:807–16; doi: 10.17179/excli2016-777.
- Satoh K. Serum lipid peroxide in cerebrovascular disorders determined by a new colorimetric method. *Clin Chim Acta*, 1978; 90:37–43; doi: 10.1016/0009-8981(78)90081-5.
- Shabbir A, Shahzad M, Ali A, Zia-Ur-Rehman M. Discovery of new benzothiazine derivative as modulator of pro- and anti-inflammatory cytokines in rheumatoid arthritis. *Inflammation*, 2016; 39:1918–29; doi: 10.1007/s10753-016-0427-y.
- Sharma MK, Sharma A, Kumar A, Kumar M. Evaluation of protective efficacy of *Spirulina fusiformis* against mercury induced nephrotoxicity in Swiss albino mice. *Food Chem Toxicol*, 2007; 45(6):879–87; doi: 10.1016/j.fct.2006.11.009.
- Silveira KD, Coelho FM, Vieira AT, Barroso LC, Queiroz-Junior CM, Costa VV, Sousa LF, Oliveira ML, Bader M, Silva TA, Santos RA, Silva AC, Teixeira MM. Mechanisms of the anti-inflammatory actions of the angiotensin type 1 receptor antagonist losartan in experimental models of arthritis. *Peptides*, 2013; 46:53–63; <https://doi.org/10.1016/j.peptides.2013.05.012>.
- Trejo E, Arellano A, Reyes O, Arroyo F, Argüello-García R, Loredo M, Tapia E, Sánchez-Lozada L, Alonso H. The beneficial effects of allixin in chronic kidney disease are comparable to losartan. *Int J Mol Sci*, 2017; 18:1980; 10.3390/ijms18091980.
- Uzunhisarcikli M, Aslanturk A, Kalender S, Apaydin FG, Bas H. Mercuric chloride induced hepatotoxic health and hematologic changes in rats: the protective effects of sodium selenite and vitamin E. *Toxicol Ind Health*, 2016; 32:1651–62; doi: 10.1177/0748233715572561.
- Yahya S, Abdelhamid A, Abd-Elhalim MM, Elsayed GH, Eskander E. The effect of newly synthesized progesterone derivatives on apoptotic and angiogenic pathway in MCF-7 breast cancer cells. *Steroids*, 2017; 126; doi:10.1016/j.steroids.2017.08.002.
- Yanagisawa H. HgCl<sub>2</sub>-induced acute renal failure and its pathophysiology. *Nihon Eiseigaku Zasshi*, 1998; 52(4):618–23; doi: 10.1265/jjh.52.618.
- Zakia MEA, Soliman HA, Hiekal OA, Rashad AE. Pyrazolopyranopyrimidines as a class of anti-inflammatory agents. *Z Naturforsch C J Bioscie*, 2006; 61:1–5; doi: 10.1515/znc-2006-1-201.
- Zhang H, Tan X, Yang D, Lu J, Liu B, Baiyun R, Zhang Z. Dietary luteolin attenuates chronic liver injury induced by mercuric chloride via the Nrf2/NF-κB/P53 signaling pathway in rats. *Oncotarget*, 2017; 8(25):40982–93; <https://doi.org/10.18632/oncotarget.17334>.

#### How to cite this article:

Mohamed SH, El-Kady DS, ElMegeed GA, El-kassaby MI, Farrag AH, Abdelhalim MM, Ali NA. The efficacy of novel heterocyclic activators against mercuric chloride-induced acute renal failure in rats. *J Appl Pharm Sci*, 2023; 13(04): 070–083.